

Effects of pressure on high-temperature dislocation creep in olivine

SHUN-ICHIRO KARATO† and HAEMYEONG JUNG‡

Department of Geology and Geophysics, University of Minnesota, Minneapolis, Minnesota 55455, USA

[Received 22 January 2001 and accepted in revised form 14 August 2001]

ABSTRACT

Effects of pressure on high-temperature, dislocation creep in olivine ((Mg, Fe)₂SiO₄) aggregates have been determined under both water-poor ('dry') and water-saturated ('wet') conditions. New experimental data were obtained at pressures of 1–2 GPa under 'dry' and 'wet' conditions using a newly developed high-resolution dislocation density measurement technique to estimate the creep strength. These data are compared with previous data at lower and higher pressures to determine the pressure dependence of high-temperature dislocation creep in olivine aggregates. We find that the creep strength σ under 'dry' conditions increases monotonically with increasing pressure, whereas the creep strength under 'wet' conditions changes with pressure in a non-monotonic fashion: it first decreases rapidly with increasing pressure and then becomes less sensitive to pressure at above 1 GPa. Such behaviour can be described by the following formula:

$$\dot{\epsilon}_{d,w} = A_{d,w} f_{H_2O}^r(T, P) \exp\left(\frac{-(E_{d,w}^* + PV_{d,w}^*)}{RT}\right) \sigma^n,$$

where the subscripts d and w refer to parameters for 'dry' and 'wet' conditions respectively. The present study gives $A_d = 10^{6.1 \pm 0.2} \text{ s}^{-1} (\text{MPa})^{-n}$, $E_d^* = 510 \pm 30 \text{ kJ mol}^{-1}$, $V_d^* = 14 \pm 2 \text{ cm}^3 \text{ mol}^{-1}$ and $r = 0$ for 'dry' conditions, and $A_w = 10^{2.9 \pm 0.1} \text{ s}^{-1} (\text{MPa})^{-n-r}$, $E_w^* = 470 \pm 40 \text{ kJ mol}^{-1}$, $V_w^* = 24 \pm 3 \text{ cm}^3 \text{ mol}^{-1}$ and $r = 1.20 \pm 0.05$ for 'wet' conditions ($n = 3.0 \pm 0.1$ for both 'dry' and 'wet' conditions). The large activation volume for 'wet' conditions can be interpreted as due to the additional contribution from the activation volume for dissolution of OH in the olivine structure ($V_{OH}^* \approx 11 \text{ cm}^3 \text{ mol}^{-1}$). The value of r (≈ 1.2) is consistent with a model in which creep in olivine is rate controlled by the motion of positively charged jogs through the diffusion of silicon via an interstitial mechanism.

§1. INTRODUCTION

Pressure is one of the important thermodynamic parameters that controls the plastic flow of materials (Sherby *et al.* 1970, Frost and Ashby 1982, Karato 1998).

† Present address: Department of Geology and Geophysics, Yale University, New Haven, Connecticut 06520, USA. Email: Shun-ichiro.karato@yale.edu.

‡ Present address: Institute of Geophysics and Planetary Physics, University of California, Riverside, California 92521, USA.

Although pressure effects on plastic flow are small at low pressures, its effects become significant when pressure exceeds a few per cent of the bulk modulus of a given material. Such high pressures are often encountered in materials synthesis (for example Strong and Wentorf (1972)) as well as in the deep interiors of planets (for example Ringwood (1975)). Thus, understanding the effects of pressure on plastic flow of solids is critical to both materials science and planetary science. The manner in which the plastic flow properties of materials change with pressure is dependent on microscopic mechanisms. Therefore studies of effects of pressure not only provide data sets to estimate the magnitude of pressure effects but also help to constrain the microscopic mechanisms of plastic deformation. This paper reports such a study on ferromagnesian silicate olivine ($\text{Mg, Fe}_2\text{SiO}_4$), one of the most abundant materials in the shallow portions of terrestrial planets (for example Ringwood (1975)).

The pressure dependence of plastic flow is usually described by a flow law of the form (for example Frost and Ashby 1982)

$$\dot{\epsilon}(T, P) = A\sigma^n \exp\left(-\frac{E^* + PV^*}{RT}\right), \quad (1)$$

where $\dot{\epsilon}$ is the strain rate, A is a constant, σ is the stress, n is the stress exponent, E^* is the activation energy, V^* is the activation volume, P is the pressure, T is the temperature and R is the gas constant. Such a relation would imply that the strain rate (the creep strength) changes monotonically with pressure. However, some complications may arise in materials in which the concentration of defects is also a strong function of pressure through its effects on the chemical potential of the defects. In such cases, the creep strength may change with pressure in a more complicated fashion (Karato 1989).

Most previous experimental studies on deformation of olivine have assumed the functional form (1) and determined the activation volume V^* . The reported values of V^* for olivine range from 5 to $27 \text{ cm}^3 \text{ mol}^{-1}$ (Green and Borch 1987, Bussod *et al.* 1993, Karato and Rubie 1997), indicating the difficulties in obtaining reliable results on creep strength under high pressures.

In addition to this difficulty, there is an additional complication. In contrast with these earlier results, the recent study by Mei and Kohlstedt (2000) reported an *increase* in strain rate (*decrease* in creep strength) with increasing pressure when olivine was deformed in the presence of water; this would imply a negative V^* which is not consistent with known defect-related properties of olivine (for example Karato (1989)). This suggests that equation (1) may not be appropriate in the case where water is present. It appears that more detailed studies under high pressures are needed to understand the pressure dependence of plastic deformation of this material. In this paper, we report new results of measurements of plastic flow strength of olivine under high pressure with and without the presence of water. We analyse the results using a new formulation of the pressure dependence of plastic flow and discuss the implications of this formulation for microscopic mechanisms of deformation.

§2. EXPERIMENTAL PROCEDURE

We deformed olivine aggregates (the starting material is San Carlos olivine; $[\text{Fe}]/([\text{Fe} + \text{Mg}]) = 0.1$; melting temperature $T_m = 2100 \text{ K}$; bulk modulus $K = 120 \text{ GPa}$ at 1–2 GPa confining pressure using a solid-medium deformation apparatus (the Griggs apparatus (Tullis and Tullis 1986))) and compared our results with those obtained at lower pressures (from 0.1 to 0.45 GPa (Karato *et al.* 1986,

Mei and Kohlstedt 2000)) and at a higher pressure (about 15 GPa (Karato and Rubie 1997)).

Deformation experiments were conducted either under water-poor ('dry') conditions or water-saturated ('wet') conditions. The oxygen fugacity was buffered by Ni–NiO reaction. 'Wet' experiments were conducted using a talc + brucite mixture as a source of water (for details see Jung and Karato (2001a)). Both talc and brucite will break down during heating to generate free water, the amount of which significantly exceeds the amount of water to saturate the olivine samples. All deformed samples were analysed by Fourier transform infrared spectroscopy to measure their water content. In experiments under 'dry' conditions, the starting materials were synthesized at 300 MPa confining pressure and temperature of 1473 K and dried in a CO–CO₂ gas mixture at 1473 K for about 20 h to remove the residual water further. All the materials in a sample assembly were carefully dried prior to each experiment (pyrophyllite was fired at 1223 K for 2 h). The water content in 'dry' samples is less than about 100 ppm H/Si. The water content in 'wet' samples is close to the solubility limit (about 1300 ppm H/Si at $P = 2$ GPa) determined by Kohlstedt *et al.* (1996). The deformation experiments were conducted in simple shear at constant strain rate at $T = 1473$ or 1573 K to shear strains of about 0.5–4. The uncertainties of temperature in our experiments was approximately ± 20 K, which is caused mostly by the temperature gradient in a sample assembly. The microstructures of all deformed samples were observed under an optical microscope as well as a scanning electron microscope. Dynamic recrystallization occurred in most cases and the grain size reached a steady-state value corresponding to a given stress (Jung and Karato 2001a). Previous studies on olivine showed that, after the completion of dynamic recrystallization, the mechanical behaviour becomes nearly steady state (for example Zhang *et al.* (2000)). Scanning electron microscopy observations show evidence of dislocation creep including subboundary formation and lattice preferred orientations (figure 1) (Jung and Karato 2001b). Consequently, we consider that the strength of our samples determined in the present experiments represents that of dislocation creep in a (nearly) steady state.

The strength of a sample could in principle be measured from the reading of an external load cell after corrections for the friction between the piston and surrounding materials. However, friction corrections in the Griggs apparatus are known to contain large uncertainties (Gleason and Tullis 1993). Significant improvements in the strength measurements have been made through the use of a soft pressure medium (for example Green and Borch (1987) and Tingle *et al.* (1993)), but the correction for the friction is still large and pressure dependent and this technique is not suitable for the present purpose. Therefore we did not use the reading of the external load cell to infer the sample strength in this study. Instead, we used the dislocation densities of deformed samples to infer the stress magnitude that had acted on the sample. The physical basis for this is the relation (for example Bailey and Hirsch (1960))

$$\rho = \alpha b^{-2} \left(\frac{\sigma}{\mu} \right)^m, \quad (2)$$

where ρ is dislocation density, b is the length of the Burgers vector, α is a non-dimensional constant of order unity, σ is the differential stress, μ is the shear modulus and m is a constant. All the materials parameters in this relation are

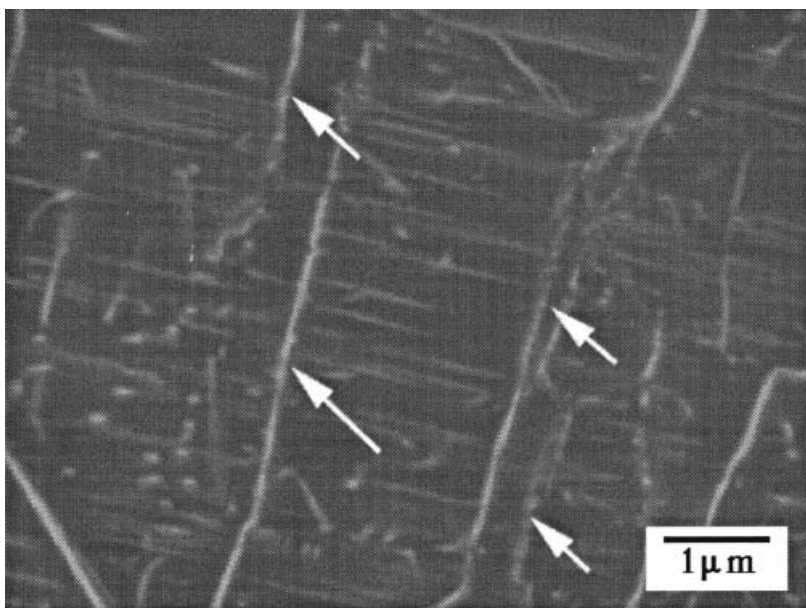


Figure 1. A scanning electron micrograph of a deformed olivine (back-scattered electron image of a sample deformed at $P = 2$ GPa, and $T = 1473$ K at $\dot{\epsilon} = 10^{-4}$ s $^{-1}$). Individual dislocations and subgrain boundaries are decorated by oxidation and are seen as bright lines owing to a higher concentration of iron (Karato 1987). Subboundaries are shown by white arrows. The total length of dislocations (excluding those in subboundaries) was measured to estimate the stress magnitude.

insensitive to pressure at least in the pressure range of this study. The calibration of this relation was made using samples that were deformed at known stress levels at a lower pressure ($P = 300$ MPa) in a gas-medium deformation apparatus under both ‘dry’ and ‘wet’ conditions. For each sample, we determined the dislocation density from the total length of dislocation lines measured with the scanning electron microscopy technique (Karato 1987, Jung and Karato 2001a) and used equation (2) to estimate the strength of that sample. A total of 25–30 grains (a volume of about 3000–6000 μm^3) was used for each sample. The results are shown in figure 2. The uncertainties in stress estimate are evaluated from the calibrations as well as the scatter in the dislocation density in a single sample and are about ± 10 –15%. Adding the uncertainties of strength estimate caused by the uncertainties in temperatures and pressure, we consider the uncertainties in strength estimates are about $\pm 20\%$.

The results are summarized in table 1 together with the results from other studies. In comparing the results from other studies, we made a correction for the deformation geometry assuming that our samples show isotropic plasticity. The difference in strain rates is corrected by assuming the stress exponent to be $n = 3.0 \pm 0.1$ (Mei and Kohlstedt 2000). Also the results are corrected for the effects of different temperatures assuming an activation energy $E_w^* = 470 \pm 40$ kJ mol $^{-1}$ for ‘wet’ experiments and $E_d^* = 510 \pm 30$ kJ mol $^{-1}$ for ‘dry’ experiments (we used the subscripts w and d to indicate that these values correspond to ‘wet’ and ‘dry’ conditions respectively).

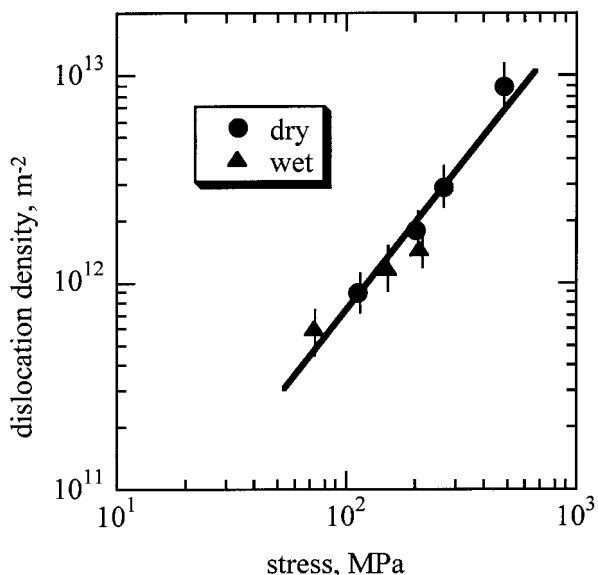


Figure 2. Dislocation density versus stress relationship for olivine determined by the deformation experiments using a gas-medium apparatus (Karato *et al.* 1986, Zhang *et al.* 2000) and the dislocation density measurements using scanning electron microscopy (this study (see also Jung and Karato (2001a))): (●), data under ‘dry’ conditions; (▲), data under ‘wet’ conditions. The least-squares fit yields $\rho = \beta\sigma^m$ with $\log_{10} \beta = 9.04 \pm 0.41$ and $m = 1.41 \pm 0.16$ where the units are reciprocal square metres for dislocation density and multipascals for stress.

Table 1. Creep strength of olivine. All the data are normalized to a strain rate of 10^{-4} s^{-1} and a temperature of 1473 K. The error bars are about $\pm 0.5\%$ for the data from Karato *et al.* (1986) and Mei and Kohlstedt (2000), about $\pm 20\%$ for the data from this study and about $\pm 30\%$ for the data from Karato and Rubie (1997). The actual temperatures of experiments were 1573 K for the work of Karato *et al.* (1986), 1473–1573 K for the work of Mei and Kohlstedt (2000), 1473 K (‘wet’) or 1573 K (‘dry’) for the work in this study and 1900 K for the work of Karato and Rubie (1997).

Pressure (GPa)	Water ^a	Strength (MPa)	Source
0.1	‘wet’	358	Mei and Kohlstedt (2000)
0.3	‘wet’	265	Mei and Kohlstedt (2000)
0.3	‘dry’	493	Mei and Kohlstedt (2000)
0.3	‘wet’	272	Karato <i>et al.</i> (1986)
0.3	‘dry’	538	Karato <i>et al.</i> (1986)
0.45	‘wet’	227	Mei and Kohlstedt (2000)
1.0	‘wet’	184	This study
1.0	‘wet’	172	This study
2.0	‘wet’	191	This study
2.0	‘wet’	184	This study
2.0	‘dry’	1063	This study
2.0	‘dry’	1015	This study
15	‘dry’	96000	Karato and Rubie (1997)

^a ‘Wet’ means water saturated, and ‘dry’ means water poor (see text for details).

§3. RESULTS

The results for ‘dry’ conditions are summarized in figure 3, showing that equation (1) holds with a constant activation volume $V_d^* = 14 \pm 2 \text{ cm}^3 \text{ mol}^{-1}$ and the pre-exponential term $A_d = 10^{6.1 \pm 0.2} \text{ s}^{-1} (\text{MPa})^{-n}$. Although the experimental errors are large at higher pressures, the activation volume V_d^* under ‘dry’ conditions is well constrained by the experimental data because of the large range of pressures. This result agrees well with previous work (Karato and Rubie 1997) and there is no indication of strong pressure dependence of activation volume as claimed by Green and Borch (1987).

Figure 4 shows the results under ‘wet’ conditions using the same type of diagram. It is seen that under ‘wet’ conditions, the strength of olivine samples first decreases with increasing pressure and then becomes insensitive to pressure at higher pressures. Therefore a simple formulation such as equation (1) cannot be used to analyse the mechanical data for olivine under ‘wet’ conditions. This behaviour suggests that more than a single factor affect the pressure dependence of creep strength, and one needs at least two parameters to characterize the pressure dependence of creep strength. Consequently a wide range of pressure must be explored in experimental studies. Thus, although mechanical data at lower pressures can be obtained with higher resolution (Mei and Kohlstedt 2000), such data are insensitive to V_w^* and hence cannot be used to characterize the pressure effects fully under ‘wet’ conditions.

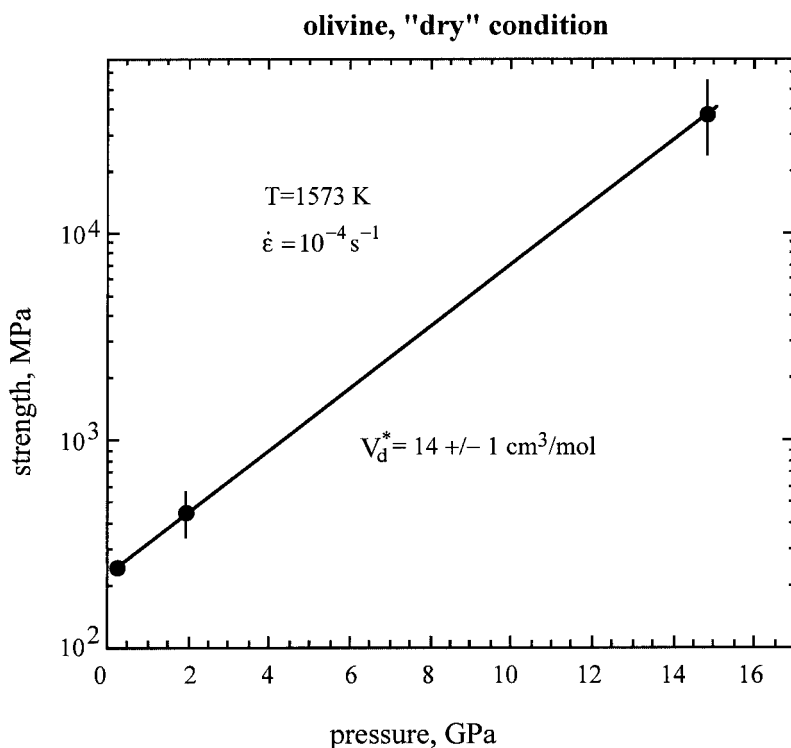


Figure 3. Creep strength versus pressure relationship for olivine under ‘dry’ conditions. All the data are normalized to a strain rate of 10^{-4} s^{-1} and a temperature of 1573 K. The straight line shows the result of the least-squares fit, yielding an activation volume of $V_d^* = 14 \pm 1 \text{ cm}^3 \text{ mol}^{-1}$.

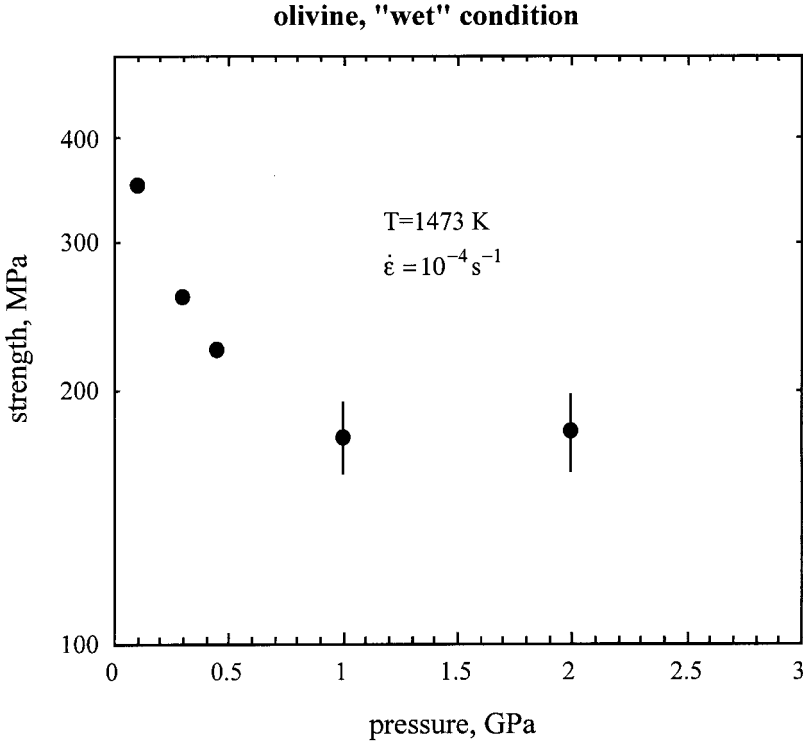


Figure 4. Creep strength versus pressure relationship for olivine under 'wet' conditions. All the data are normalized to a strain rate of 10^{-4} s^{-1} and a temperature of 1473 K. The creep strength first decreases with increasing pressure and then becomes insensitive to pressure.

The rate of plastic deformation of silicates such as olivine depends on temperature and pressure directly through the temperature and pressure dependences of defect mobility, but also indirectly through the temperature and pressure dependences of concentration C_{OH} of water-related defects. C_{OH} depends on water fugacity $f_{\text{H}_2\text{O}}$, which in turn depends on temperature and pressure. Thus, plastic flow under a water-rich ('wet') environment may be described by (for example Karato 1989, Mei and Kohlstedt 2000)

$$\dot{\epsilon}(T, P, C_{\text{OH}}) = A_w f_{\text{H}_2\text{O}}^r(T, P) \sigma^n \exp\left(-\frac{E_w^* + PV_w^*}{RT}\right), \quad (3)$$

where A_w and r are constants and in general the activation energy E_w^* and volume V_w^* can be different from those under 'dry' conditions. The water fugacity $f_{\text{H}_2\text{O}}$ increases with increasing pressure, but the term $\exp[-(E_w^* + PV_w^*)/RT]$ decreases with increasing pressure for a positive activation volume. The first term $f_{\text{H}_2\text{O}}^r$ dominates at low pressures, whereas the second term $\exp[-(E_w^* + PV_w^*)/RT]$ dominates at higher pressures. Therefore, a non-monotonic dependence of creep strength on pressure is expected under 'wet' conditions.

The results under 'wet' conditions were analysed assuming a creep constitutive relation of the form (3) (figure 5). We calculated the water fugacity using the thermodynamic data of Pitzer and Sterner (1994) and determined the parameters

olivine, "wet" condition

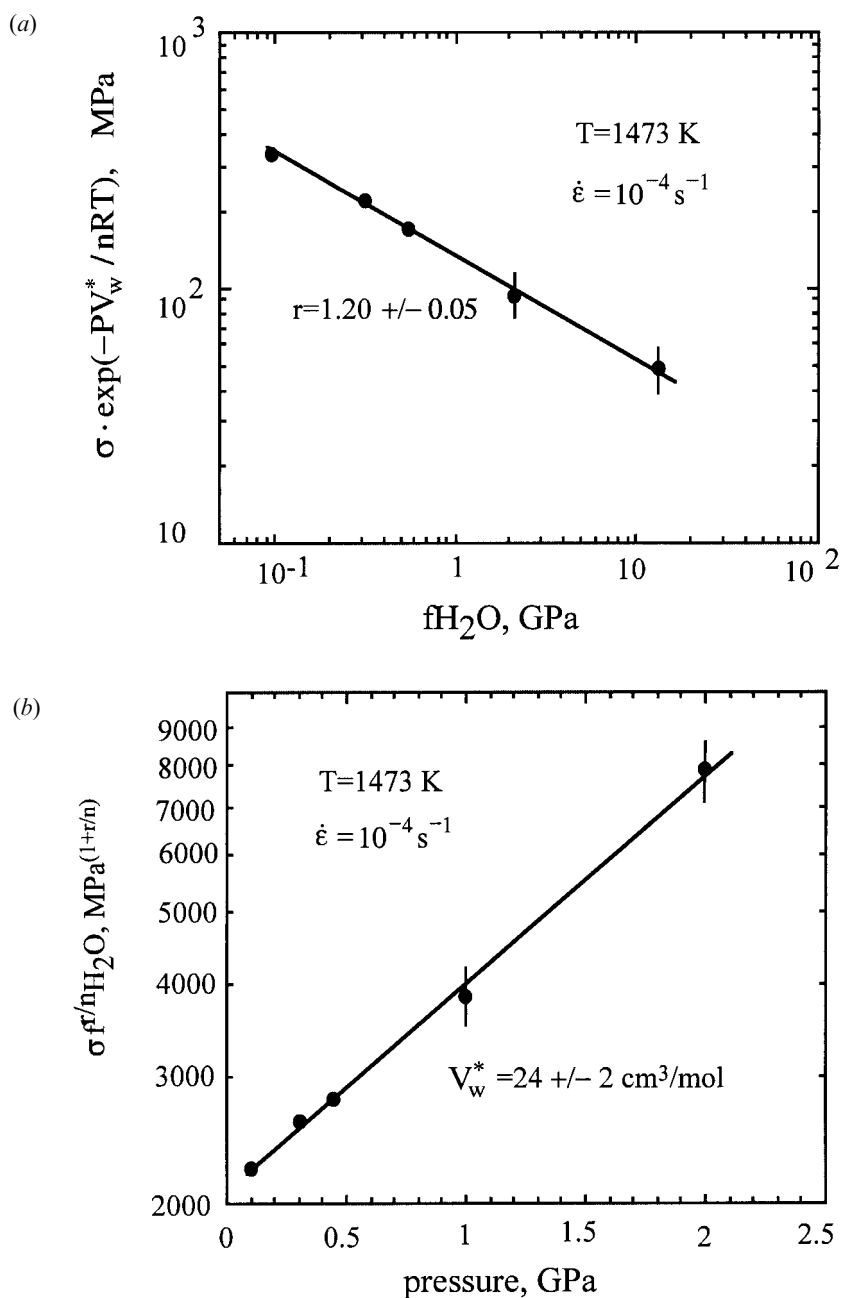


Figure 5. The creep strength as a function of (a) water fugacity and (b) pressure. The parameters r and V_w^* are determined by an iterative least-squares fit. (a) Creep strength versus water fugacity relationship under 'wet' conditions. The creep strength corrected for the activation volume effect (i.e. $\sigma \exp(-PV_w^*/nRT)$) is plotted against water fugacity. The slope gives $r = 1.20 \pm 0.05$. (b) Creep strength versus pressure relationship under 'wet' conditions after correction for the water fugacity effects ($\sigma f^{1/r} / H_2O$). The slope yields an activation volume of $V_w^* = 24 \pm 3 \text{ cm}^3 \text{ mol}^{-1}$.

A_w , r and V_w^* by an iterative least-squares fit to obtain $A_w = 10^{2.9 \pm 0.1} \text{ s}^{-1} (\text{MPa})^{-r-n}$, $r = 1.20 \pm 0.05$ and $V_w^* = 24 \pm 3 \text{ cm}^3 \text{ mol}^{-1}$. The somewhat higher uncertainty is the result of a smaller pressure range and reflects the uncertainties in temperature, pressure as well as stress.

§4. DISCUSSION

Despite large uncertainties in the mechanical data obtained with the solid-medium Griggs apparatus, non-monotonic variation in the creep strength of olivine with pressure under ‘wet’ conditions is well documented by the present study. The good fit of the present data set to the functional form (3) shown in figure 5 suggests that this formulation is valid for the flow law of olivine under ‘wet’ conditions. The non-monotonic dependence of strength on pressure under ‘wet’ conditions found in this work is therefore interpreted as a consequence of the combined effects of change in water fugacity with pressure and change in activation enthalpy for defect motion. The value of r can be used to infer the defects involved in plastic deformation (Karato 1989, Yan 1992, Mei and Kohlstedt 2000).

Yan (1992) (see also Karato (1989)) analysed the point-defect chemistry of olivine under ‘wet’ conditions and showed that the charge neutrality condition for olivine changes from $[\text{Fe}^\bullet] = 2[\text{V}_M'']$ to $[\text{Fe}^\bullet] = [\text{H}_M']$ or to $[\text{Fe}^\bullet] = [(\text{OH})_I']$ as the fugacity of water is increased (the Kröger–Vink (1956) notation of point defects is used). The results are summarized in table 2. The value of r ($= 1.20 \pm 0.05$) determined in this study is close to $r = +5/4$ predicted for a case where creep rate is controlled by a motion of positively charged jogs J^\bullet through the diffusion of silicon

Table 2. Dependence of concentration of point defects in olivine on the fugacity of water (after Karato (1989) and Yan (1992)). Charge neutrality conditions of either $[\text{Fe}^\bullet] = [\text{H}_M']$ or $[\text{Fe}^\bullet] = [(\text{OH})_I']$ are assumed. The parameter r is defined by $[\text{X}] \propto f_{\text{H}_2\text{O}}^r$ or by $\dot{\epsilon} \propto f_{\text{H}_2\text{O}}^r$, where $[\text{X}]$ is the concentration of defect X.

	Defect	r for defect concentration	r for strain rate ^a		
			J^\bullet	J^x	J'
M (Mg or Fe)	$\text{M}_I^{\bullet\bullet}$	+1/2			
	V_M''	-1/2			
O	O_I''	-1/2	-1/4	-1/2	-3/4
	$\text{V}_O^{\bullet\bullet}$	+1/2	+3/4	+1/2	+1/4
Si	$\text{Si}_I^{\bullet\bullet\bullet\bullet}$	+1	+5/4	+1	+3/4
	V_{Si}'''	-1	-3/4	-1	-5/4
Jog	J^\bullet	+1/4			
	J^x	0			
	J'	-1/4			

^a The dependence of the strain rate on water fugacity is calculated assuming that strain rate is proportional to (defect concentration) × (concentration of jogs). Three models corresponding to a given point defect include those controlled by motion of positively charged, neutral or negatively charged jogs through diffusion of some ions. Creep in $(\text{Mg, Fe})_2\text{SiO}_4$ is likely to be controlled by diffusion of either oxygen or silicon. Therefore only the values of r corresponding to models involving these defects are shown in this table.

via an interstitial mechanism (in this case, the strain rate is proportional to $[\text{Si}_i^{\bullet\bullet\bullet}][\text{J}^{\bullet}] \propto f_{\text{H}_2\text{O}}^{5/4}$). This model is also consistent with other observations including the dependence of the dislocation recovery rate on oxygen fugacity and oxide activity (Yan 1992). This mechanism is consistent with the results on measurements of silicon diffusion in olivine which indicate that it occurs through an interstitial mechanism (Houlier *et al.* 1990). The notion that dislocations in $(\text{Mg}, \text{Fe})_2\text{SiO}_4$ olivine have positively charged jogs is also consistent with the fact that this material usually behaves like a p-type semiconductor (Karato 1974) in which dislocations and grain boundaries tend to be positively charged (Eshelby *et al.* 1958, Menezes and Nix 1974).

Given the relation between water fugacity and strain rate determined above and using the relation $C_{\text{OH}} \propto f_{\text{H}_2\text{O}} \exp[-(E_{\text{OH}}^* + PV_{\text{OH}}^*)/RT]$ (E_{OH}^* and V_{OH}^* are the activation energy and the volume respectively for dissolution of OH in olivine) for an open system (Kohlstedt *et al.* 1996), we obtain

$$\dot{\epsilon}(T, P, C_{\text{OH}}) = A_w' C_{\text{OH}}^r \sigma^n \exp\left(-\frac{E_w^{*'} + PV_w^{*'}}{RT}\right), \quad (4)$$

where $E_w^{*'}$ and $V_w^{*'}$ are the activation energy and activation volume respectively for defect (dislocation) migration. Therefore, in an open system, the temperature and pressure dependences of creep under 'wet' conditions include the temperature and pressure dependences of water content $C_{\text{OH}}(T, P)$ as well as the activation volume for defect migration. Thus,

$$E_w^* = rE_{\text{OH}}^* + E_w^{*'}. \quad (5)$$

and

$$V_w^* = rV_{\text{OH}}^* + V_w^{*'}. \quad (6)$$

Using the value of $V_{\text{OH}}^* = 10.6 \text{ cm}^3 \text{ mol}^{-1}$ (Kohlstedt *et al.* 1996), we obtain $V_w^{*' = 11 \pm 3 \text{ cm}^3 \text{ mol}^{-1}$. Thus the observed large activation volume is in part due to the contribution from V_{OH}^* . Similarly, from equation (5) and $E_{\text{OH}}^* = 50 \pm 5 \text{ kJ mol}^{-1}$ (Zhao *et al.* 2001), we get $E_w^{*' = 410 \pm 40 \text{ kJ mol}^{-1}$.

We note that both the activation energy and the activation volume of defect mobility under 'wet' conditions are less than those under 'dry' conditions ($V_d^* = 14 \pm 2 \text{ cm}^3 \text{ mol}^{-1}$ and $E_d^* = 510 \pm 30 \text{ kJ mol}^{-1}$). This difference is probably due to the difference in deformation mechanisms between 'wet' and 'dry' conditions. For example, the relative strength of different slip systems in olivine is likely to change as water fugacity increases (Mackwell *et al.* 1985, Jung and Karato 2001b). This will change the rate-controlling slip system from $[001](010)$ under 'dry' conditions to another system (e.g. $[100](001)$) under 'wet' conditions.

When the system under consideration is closed with respect to water, and materials are undersaturated with water, then the concentration of OH in olivine will not change with temperature and pressure. In this case, equation (4) must be used with C_{OH} being a constant and the activation energy and activation volume are different from those in an open system.

In a more general case, where a range of water fugacities covers from 'dry' to 'wet' conditions, we may add strain rates for 'dry' rheology (equation (1)) and those for 'wet' rheology (equation (3)) to obtain an actual strain rate. The underlying assumption is that the processes causing deformation under 'dry' conditions and

those under ‘wet’ conditions are independent, which is supported by a model of point-defect chemistry (for example Karato 1989). All the parameters needed to calculate the strain rate (or the strength) of olivine under a given condition are summarized in tables 3 and 4.

Our results under ‘dry’ conditions ($V_d^* = 14 \pm 1 \text{ cm}^3 \text{ mol}^{-1}$) are different from some previous results such as those of Green and Borch (1987), who obtained $V^* = 27 \text{ cm}^3 \text{ mol}^{-1}$ at nearly identical conditions using the same type of apparatus, but using a different technique for strength measurements. Consequently, we consider that the cause of this difference is partly due to the difference in the technique used to measure the strength; the measurements of pressure dependence of strength using an external load cell may be affected by the pressure dependence of friction. In addition, the thermodynamic environment, and in particular the water fugacity, in their experiments was not well characterized.

Mei and Kohlstedt (2000) also attempted to determine r to infer the mechanisms of plastic flow in olivine. In the pressure range explored by Mei and Kohlstedt (2000)

Table 3. Creep law parameters for olivine aggrates for an open system:

$$\dot{\epsilon}(T, P) = \left[A_d \exp\left(-\frac{E_d^* + PV_d^*}{RT}\right) + A_w f_{\text{H}_2\text{O}}(T, P) \exp\left(-\frac{E_w^* + PV_w^*}{RT}\right) \right] \sigma^n.$$

Parameter	Value	Source
A_w	$10^{2.9 \pm 0.1} \text{ s}^{-1} (\text{MPa})^{-n-r}$	This study
A_d	$10^{6.1 \pm 0.2} \text{ s}^{-1} (\text{MPa})^{-n}$	This study
r	1.20 ± 0.05	This study
E_w^*	$470 \pm 40 \text{ kJ mol}^{-1}$	Mei and Kohlstedt (2000)
E_d^*	$510 \pm 30 \text{ kJ mol}^{-1}$	Mei and Kohlstedt (2000)
V_w^*	$24 \pm 3 \text{ cm}^3 \text{ mol}^{-1}$	This study
V_d^*	$14 \pm 2 \text{ cm}^3 \text{ mol}^{-1}$	This study
n	3.0 ± 0.1	Mei and Kohlstedt (2000)

Table 4. Creep law parameters for olivine aggrates for a closed system:

$$\dot{\epsilon}(T, P, C_{\text{OH}}) = \left[A_d \exp\left(-\frac{E_d^* + PV_d^*}{RT}\right) + A_w' C_{\text{OH}} \exp\left(-\frac{E_w'^* + PV_w'^*}{RT}\right) \right] \sigma^n.$$

Parameter	Value	Source
A_w'	$10^{0.56 \pm 0.02} \text{ s}^{-1} (\text{MPa})^{-n}$	This study
A_d	$10^{6.1 \pm 0.2} \text{ s}^{-1} (\text{MPa})^{-n}$	This study
r	1.20 ± 0.05	This study
$E_w'^*$	$410 \pm 40 \text{ kJ mol}^{-1}$	This study
E_d^*	$510 \pm 30 \text{ kJ mol}^{-1}$	Mei and Kohlstedt (2000)
$V_w'^*$	$11 \pm 3 \text{ cm}^3 \text{ mol}^{-1}$	This study
V_d^*	$14 \pm 2 \text{ cm}^3 \text{ mol}^{-1}$	This study
n	3.0 ± 0.1	Mei and Kohlstedt (2000)

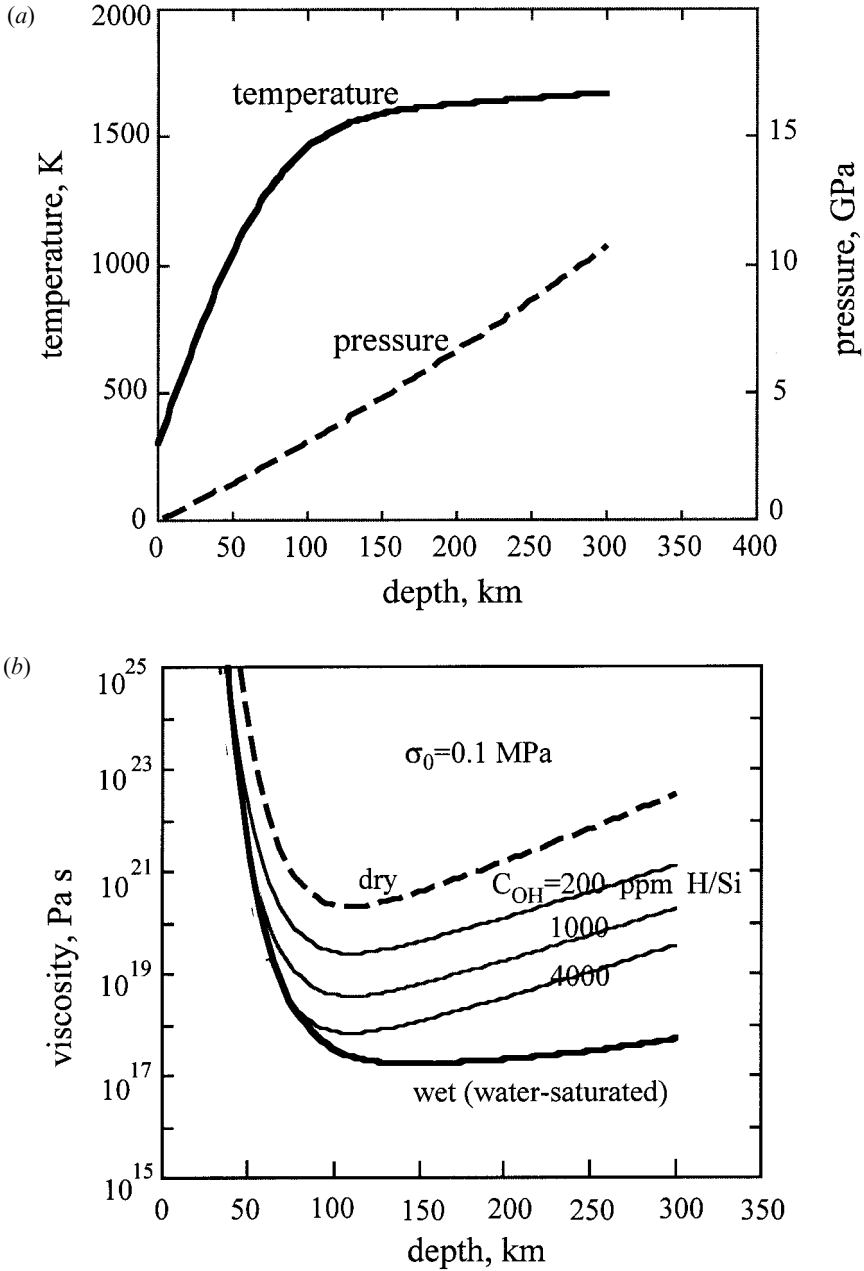


Figure 6. Viscosity–depth profiles for (b) the upper mantle of the Earth for (a) the pressure–depth and temperature–depth profiles for the standard model of the Earth. The stress is assumed to be constant with depth. The viscosities η_0 for a constant stress $\sigma_0 = 0.1$ MPa are calculated. The viscosities η for other stress levels σ can be calculated from $\eta/\eta_0 = (\sigma_0/\sigma)^{n-1}$. Equation (1) or (3) was used to calculate the viscosity–depth profiles for ‘dry’ or ‘wet’ conditions respectively. The ‘dry’ profile corresponds to the water-poor case, and the ‘wet’ profile to the water-saturated case. Viscosity–depth profiles for cases where the water content C_{OH} is fixed (i.e. a closed system) are also calculated using equation (4).

(below 0.45 GPa) their data are sensitive to both r and V_w^* , but the pressure range was too narrow to determine r and V_w^* separately. Consequently they were unable to determine r and V_w^* uniquely (the value of r compatible with their data ranges from 0.69 to 1.25 when the (assumed) value of V_w^* is changed from 0 to $38 \text{ cm}^3 \text{ mol}^{-1}$).

The value of the activation volume $V_d^* = 14 \pm 2 \text{ cm}^3 \text{ mol}^{-1}$ (or $V_w^{*'} = 11 \pm 3 \text{ cm}^3 \text{ mol}^{-1}$) determined by the present study may be compared with some models. A model assuming homologous temperature scaling (for example Sherby *et al.* (1970)) yields $V^* = (E^*/T_m)(dT_m/dP)$, where T_m is the melting temperature. Using the experimental results of melting temperature of olivine (Ohtani and Kumazawa 1981), one obtains $V_d^* = 11 \text{ cm}^3 \text{ mol}^{-1}$ ($V_w^{*'} = 8 \text{ cm}^3 \text{ mol}^{-1}$). Another model is the elastic strain energy model (Keyes 1963) which predicts $V^* = (E^*/K)(2\gamma - \frac{2}{3})$, where γ is the Grüneisen parameter. This model yields $V_d^* = 7 \text{ cm}^3 \text{ mol}^{-1}$ ($V_w^{*'} = 5 \text{ cm}^3 \text{ mol}^{-1}$). Both of these empirical models predict rather small activation volumes. The observed large activation volume may imply a large volume expansion associated with the formation of a Frenkel pair of $V_{\text{Si}}^{''''}$ and $\text{Si}_\text{I}^{\bullet\bullet\bullet}$ involved in silicon diffusion. The formation of a silicon vacancy ($V_{\text{Si}}^{''''}$) is likely to result in the expansion of the Si–O₄ tetrahedron because of large repulsive forces between the four oxygen ions after the removal of Si^{4+} , and the formation of a silicon interstitial ion $\text{Si}_\text{I}^{\bullet\bullet\bullet}$ could also result in a volume expansion of a crystal. One of the difficulties in this interpretation, however, is that the activation volume of silicon diffusion in olivine was reported to be $V^* \approx -2 \text{ cm}^3 \text{ mol}^{-1}$ (Béjina *et al.* 1997). If this is indeed the activation volume for silicon diffusion, then one has to invoke a very large positive activation volume for jog formation.

We emphasize that the use of a formulation (equation (3) or (4)) that is consistent with the microscopic physics is important in analysing the pressure dependence of plastic deformation. In the analysis of experimental data such a physically sensible parametrization is critical when one wants to extrapolate the results beyond the range of parameters that have been explored. For example, if a simpler version of flow law such as equation (1) were used to analyse the data obtained in this work, this would result in a negative activation volume under ‘wet’ conditions. The extrapolation of results with such a formulation would predict exceedingly low viscosities in the deep upper mantle of the Earth, which is obviously not justified.

To illustrate some geological applications, we calculated viscosity–depth profiles for the upper mantle of the Earth assuming a typical temperature–depth relationship (figure 6) assuming that stress is independent of depth. The viscosity η is defined by $\eta \equiv \sigma/\dot{\epsilon}$ and is dependent on stress as $\eta/\eta_0 = (\sigma_0/\sigma)^{n-1}$, where η_0 and σ_0 are the reference viscosity and the reference stress respectively. Viscosity–depth profiles were calculated for ‘wet’ and ‘dry’ cases as well as for some values of C_{OH} . It is seen that a variation in OH content can result in a significant change in viscosity, by more than four orders of magnitude.

ACKNOWLEDGEMENTS

This research was supported by National Science Foundation grants EAR-9903087 and EAR-0001955. H. Jung was supported by the University of Minnesota Doctoral Dissertation Fellowship. Y.-H. Zhao is thanked for the preprint by Zhao *et al.* (2001) and S. Mei for discussions.

REFERENCES

- BAILEY, J. E., and HIRSCH, P. B., 1960, *Phil. Mag.*, **5**, 485.
- BÉJINA, F., RATERSON, P., ZHANG, J., JAOLU, O., and LIEBERMANN, R. C., 1997, *Geophys. Res. Lett.*, **24**, 2597.
- BUSSOD, G. Y., KATSURA, T., and RUBIE, D. C., 1993, *Pure appl. Geophys.*, **141**, 579.
- ESHELBY, J. D., NEWBY, C. W. A., PRATT, P. L., and LIDIARD, A. B., 1958, *Phil. Mag.*, **3**, 75.
- FROST, H. J., and ASHBY, M. F., 1982, *Deformation Mechanism Maps* (Oxford: Pergamon), p. 167.
- GLEASON, G. C., and TULLIS, J., 1993, *Geophys. Res. Lett.*, **20**, 2111.
- GREEN II, H. W., and BORCH, R. S., 1987, *Acta metall.*, **35**, 1301.
- HOULIER, B., JAOLU, O., ABEL, F., and LIEBERMANN, R. C., 1990, *Phys. Earth planet. Inter.*, **62**, 329.
- JUNG, H., and KARATO, S., 2001a, *J. struct. Geol.*, **23**, 1337; 2001b, *Science*, **293**, 1460.
- KARATO, S., 1974, MSc Thesis, University of Tokyo, p. 30; 1987, *Phys. Chem. Miner.*, **14**, 245; 1989, *Rheology of Solids and of the Earth*, edited by S. Karato and M. Toriumi (Oxford University Press), p. 176; 1998, *Mater. Res. Soc. Symp. Proc.*, **499**, 3.
- KARATO, S., and RUBIE, D. C., 1997, *J. geophys. Res.*, **102**, 20 111.
- KARATO, S., PATERSON, M. S., and FITZ GERALD, J. D., 1986, *J. geophys. Res.*, **91**, 8151.
- KEYES, R. W., 1963, *Solids under Pressure*, edited by W. Paul and D. Warschauer (New York: McGraw-Hill), p. 71.
- KOHLSTEDT, D. L., KEPPLER, H., and RUBIE, D. C., 1996, *Contrib. Miner. Petrol.*, **123**, 345.
- KRÖGER, F. A., and VINK, H. J., 1956, *Solid State Physics*, edited by F. Seitz and D. Turnbull (San Diego California: Academic Press), p. 307.
- MACKWELL, S. J., KOHLSTEDT, D. L., and PATERSON, M. S., 1985, *J. geophys. Res.*, **90**, 11 319.
- MEI, S., and KOHLSTEDT, D. L., 2000, *J. geophys. Res.*, **105**, 21 471.
- MENEZES, R. A., and NIX, W. D., 1974, *Mater. Sci. Engng.*, **16**, 57.
- OHTANI, E., and KUMAZAWA, M., 1979, *Phys. Earth planet. Inter.*, **27**, 32.
- PITZER, K. S. and STERNER, S. M., 1994, *J. chem. Phys.*, **101**, 3111.
- RINGWOOD, A. E., 1975, *Composition and Petrology of the Earth's Mantle* (New York: McGraw-Hill), p. 618.
- SHERBY, O. D., ROBBINS, J. L., and GOLDBERG, A., 1970, *J. appl. Phys.*, **41**, 3961.
- STRONG, H. M., and WENTORF, R. H., JR, 1972, *Naturwissenschaften*, **59**, 1.
- TINGLE, T. N., GREEN II, H. W., YOUNG, T. E., and KOCZYNSKI, T. A., 1993, *Pure appl. Geophys.*, **141**, 523.
- TULLIS, T. E., and TULLIS, J., 1986, *Mineral and Rock Deformation*, edited by B. E. Hobbs and H. C. Heard (Washington, DC: American Geophysical Union), p. 297.
- YAN, H., 1992, MSc Thesis, University of Minnesota, 98.
- ZHANG, S., KARATO, S., FITZ GERALD, J. D., FAUL, U. H., and ZHOU, Y., 2000, *Tectonophysics*, **316**, 133.
- ZHAO, Y.-H., GINSBERG, S. B., and KOHLSTEDT, D. L., 2001, *Acta Petrol. Sinica*, **17**, 123–128.